Laser and Particle Beams (2007), *25*, 513–521. Printed in the USA.

DOI: 10.1017/S0263034607000079

Search for stable propagation of intense femtosecond laser pulses in gas

A. GIULIETTI,[1] M. GALIMBERTI,[1] A. GAMUCCI,[1] D. GIULIETTI,[1,3] L.A. GIZZI,[1] P. KOESTER,[1] L. LABATE,[1] P. TOMASSINI,[1] T. CECCOTTI,[2] P. D'OLIVEIRA,[2] T. AUGUSTE,[2] P. MONOT,[2] AND P. MARTIN[2]

[1]Intense Laser Irradiation Laboratory, IPCF-CNR, Pisa, Italy
[2]CEA-DSM/DRECAM/SPAM, Gif sur Yvette Cedex, France
[3]Department of Physics, University of Pisa, Pisa, Italy

(RECEIVED 27 November 2006; ACCEPTED 15 February 2007)

Abstract

We report and discuss experimental results on the propagation of CPA pulses of moderately relativistic intensity in gas: they evidence the effects of the precursor pedestals of the main pulse. Details of great interest were observed for the first time with high quality femtosecond 90-degree interferometry. The interferometric data are also correlated with imaging and spectroscopy data of laser pulse transmitted through the gas. The most relevant physical features are confirmed by a numerical code which simulates the laser pulse propagation self-consistently with the ionization of the gas. We found that in this regime, the propagation of the intense femtosecond pulse is basically stable apart from very weak refractive effects. In order to allow propagation at fixed intensity along an optical path larger than the Rayleigh range, we performed a first successful attempt at producing hollow plasma channels able to guide the pulse.

Keywords: Laser plasma; Laser pulse propagation; Ultra intense laser

1. INTRODUCTION

Ultra-short laser pulses have reached the petawatt peak power. When focused, such pulses can achieve ultra-relativistic intensities exceeding 10^{21} Wcm^{-2}. Some pioneering experiments on laser-matter interaction at this level of intensity already have been performed, while plenty of experimental data are now available in a variety of applications of ultra-short pulses, interacting with dense or dilute media at intensity ranging from 10^{17} Wcm^{-2} up to 10^{20} Wcm^{-2} (Patin *et al.*, 2006; Sherlock *et al.*, 2006; Chen & Wilks, 2005). This range of intensity is particularly suitable for experiments on laser acceleration of particles in plasmas either in gas jet (Mangles *et al.*, 2004, 2006; Lifshitz *et al.*, 2006; Geddes *et al.*, 2004; Faure *et al.*, 2004) or in exploded thin foils (Giulietti *et al.*, 2002, 2005; Galimberti *et al.*, 2001; Wang *et al.*, 2006; Brambrink *et al.*, 2006; Glinec *et al.*, 2005). Another class of experiments is devoted to the problem of energy transfer through a medium, like in the case of fast ignition studies for ICF. However, many of these experiments are still far from reproducibility and standardization, due to the poor knowledge of the physical conditions at which they were performed. In particular, there is a lack of data on the propagation of powerful, ultra-short pulses in gases and plasmas, though there is diffuse qualitative evidence that precursors of the main laser pulse can play a major role in the propagation of the pulse itself (Giulietti *et al.*, 1997; Gizzi *et al.*, 2001). For what concerns laser acceleration, most of the propagation instabilities, including filamentation and hosing (Najmudin *et al.*, 1999; Duda *et al.*, 1999), are expected and proved to increase their detrimental effect when the intensity of the focused laser pulse is increased. It seems then reasonable, for the transition from acceleration experiments to practical and reliable "table top" accelerators, to consider laser pulses of not extreme intensity propagating toward long acceleration paths, possibly in a guided mode (Sheng *et al.*, 2005). This idea has been supported very recently by the production of quasi-mono-energetic electron bunches of 10 s of MeV with laser pulses of duration (typically from 60 to 90 fs) larger than required at the given density by the wake-field mechanisms, at laser intensities weakly relativistic (Hidding *et al.*, 2006).

This paper presents and discusses the main results of the first systematic study on propagation of an ultra-short pulse

Address correspondence and reprint request to: A. Giulietti, Intense Laser Laboratory, IPCF-CNR, Pisa, Italy. E-mail: antonio.giulitti@ipcf.cnr.it

in a gas, at an intensity moderately relativistic ($a_0 = 1.2$). We probed with a time resolution of a few tens of femtoseconds, the *instant* production of fresh plasma by the propagating pulse front. The physics involved is further investigated by correlating these time resolved data with time-integrated data on the pulse transmitted after propagation. Section 2 is devoted to the description of the experimental setup. Section 3 presents the gas ionization data obtained from the interferograms and compares them with the numerical simulations. The contributions of the precursors of the main laser pulse are clearly identified. In Section 4, the physics of propagation is further revealed by the data from imaging and spectroscopy of the transmitted laser pulse. Section 5 is devoted to the discussion of the experimental and numerical results, as well as the perspectives for further progresses. In this context, we reports also on the production of plasma channels able to guide the laser pulse over a path length much larger than the Rayleigh range allowed by the focusing optics.

2. THE EXPERIMENT

The experiment was performed at the Saclay Laser-matter Interaction Centre (SLIC) of CEA (France) with a 10 TW UHI10 laser system, delivering 60-fs laser pulses at 800-nm from a Ti:S system operating in the chirped pulse amplification (CPA) mode. The precursors of the main pulse were carefully monitored by a third order auto-correlator, supplying the contrast of the pulse for both nano-second and picosecond time-scales. Figure 1 shows the third order auto-correlation trace of the laser pulse used in this experiment. The amplified spontaneous emission (ASE) was found to last about 1-ns before the main pulse with a contrast ratio of $\approx 10^6$, while the *pedestal* of the femtosecond pulse had a contrast ratio of $\approx 10^4$ for a few picoseconds, dropping down to 10^3 in the last picosecond before the main pulse. Recently, the contrast has been greatly improved with a "plasma mirror" technique (Doumy *et al.*, 2004).

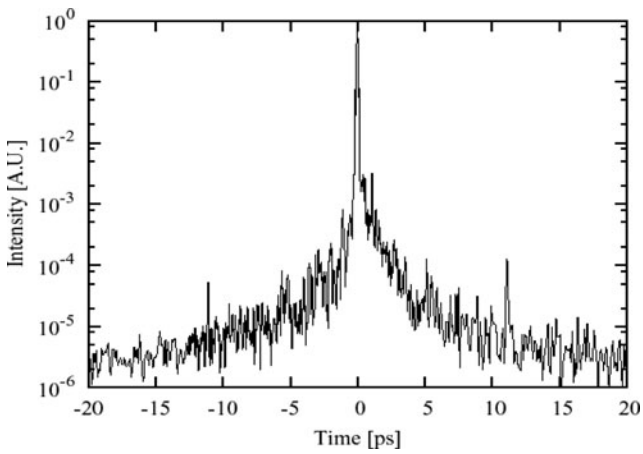

Fig. 1. Third order autocorrelation of the laser pulse.

However, the values above remain typical of most of the high power femtosecond lasers.

The schematic of the experimental setup is shown in Figure 2. The propagation was studied by focusing with an $f/5$ parabola the laser pulse in a subsonic Helium jet at the nominal intensity of 3×10^{18} Wcm^{-2}, corresponding to a moderate relativistic field of normalized parameter $a_o = 1.2$. The gas jet was delivered by a slit-like nozzle (3×0.3-mm); the laser pulse propagated along the 3-mm gas jet axis and was focused in the middle of its path. The gas jet was characterized for the purposes of this experiment at the ILIL laboratory of Istituto per i Processi Chimico-Fisici (IPCF)/CNR in Pisa. At the Intense Laser Irradiation Laboratory (ILIL), the experimental study on plasma channels, presented in Section 5, was performed. Moving the pulse path in two different distances from the nozzle, the propagation occurred at two distinct gas densities for two separate series of measurements, below and above the gas breakdown threshold for the ASE, respectively. In the following, we will call these two series bb-ASE and ab-ASE, respectively. A fraction of the femtosecond pulse was doubled in frequency and used as an optical probe perpendicular to the main pulse propagation axis in a Mach–Zehnder interferometer. Due to the low refractive index of He and the small transversal thickness of the gas layer (300-μm), the density of the neutral gas in the region of propagation could not be measured. It can be, nevertheless, inferred from the maximum electron density measured in the gas freshly ionized by the powerful CPA pulse. In this way, we found that the He density on the propagation axis was on the order of 10^{19} at/cm^3, with a difference of about 30% between the bb-ASE and the ab-ASE series of measurements, respectively. Each series of interferograms was obtained by varying the probe to main pulse delay shot by shot with a time step of 50-fs. The high reproducibility of the laser pulses allowed to "follow" the short pulse propagation, through its ionization effects, during the whole transit time in the gas, from the entrance to the exit, in about 10-ps. The large number of interferograms available, allow setting virtual "movies" of the propagation. In this paper, we present a few representative interferograms from both series.

3. THE IONIZATION DATA FROM EXPERIMENT AND SIMULATION

Figure 3 compares two interferograms together with the retrieved density maps, both showing the main pulse approaching the focal region, but at different He densities, ab-ASE (top of Fig. 3) and bb-ASE (bottom of Fig. 3), respectively. The laser light comes from the right-hand side. The position of the main pulse is indicated by a vertical bar, and was determined from the time (i.e., probe delay) of appearance of the first ionization front at the right-hand entrance of the gas jet. The electron density maps were obtained after deconvolution of the fringe pattern (Tomassini *et al.*, 2001; Tomassini & Giulietti, 2001).

https://doi.org/10.1017/S0263034607000079 Published online by Cambridge University Press

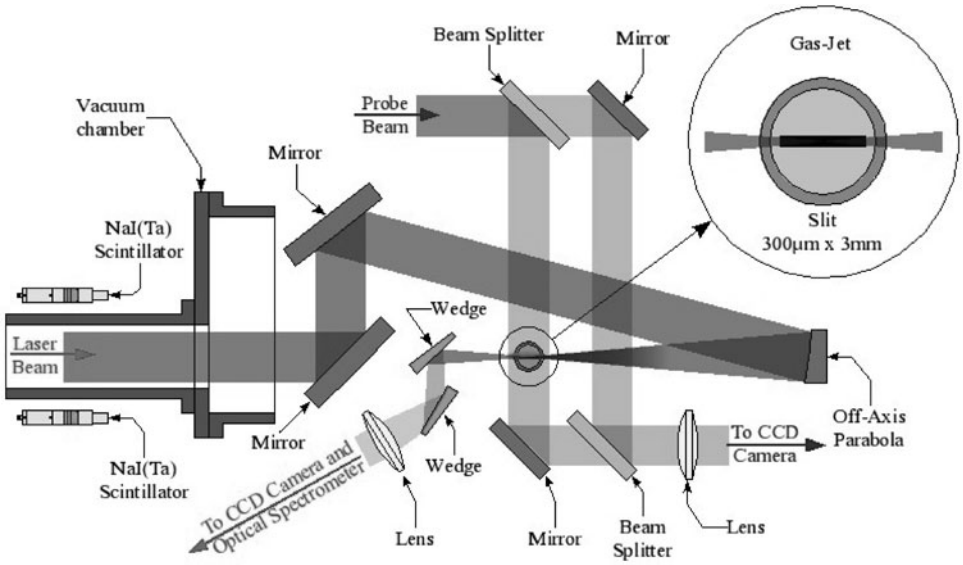

Fig. 2. Schematic of the experimental setup.

In the interferogram on top of Figure 3, the early plasma produced by the ASE is clearly visible in the central focal region. On the right-hand side there is an extended region of ionized gas, basically shaped as a cylinder of about 250-μm diameter. This plasma is due to the action of the main femtosecond pulse coming from the right. The pulse is located as shown by the vertical bar. Quite surprisingly, there is evidence for another thin plasma on the left-hand side on the axis of the plasma cylinder. From the sequence of the interferograms at different times, we know that this particular plasma appears when the main pulse approaches the focus and moves with the main plasma front at its left (i.e., in front of it). The thin plasma has a length corresponding to about 1-ps duration and then it is clearly due to the action of the picosecond pedestal of the main pulse, whose intensity (see the contrast ratio above) well exceeds the gas breakdown threshold for picosecond pulses (Ostrovskaya & Zaidel, 1974). The net change in the plasma diameter at the arrival of the main pulse evidences, an ultra-fast ionization of the gas in a diameter much larger than the waist of the focusing optics, as can be expected by the transversal intensity profile of the pulse, and the values of the intensity needed for direct ionization of the gas (by single atom multi-photon and/or tunneling processes).

The interferogram on the bottom of Figure 3 shows very similar features, but no pre-formed plasma by ASE. The picosecond pedestal still produces (close to the focus) thin plasma in front of the main pulse propagating in the gas. The electron density distribution was evaluated from the fringe pattern in the two cases, depicted in Figure 3. For the ASE pre-plasma, we found $\approx 2 \times 10^{18}\,\mathrm{cm}^{-3}$ on the axis and $\approx 1 \times 10^{19}\,\mathrm{cm}^{-3}$ at the boundary; for the main plasma produced by the CPA pulse, we found the maximum electron density to be $\approx 1.8 \times 10^{19}\,\mathrm{cm}^{-3}$ at higher He density (above threshold for ASE breakdown), $\approx 1.2 \times 10^{19}\,\mathrm{cm}^{-3}$ at lower He density; for the thin plasma produced by the picosecond pedestal, we found $\approx 8 \times 10^{18}\,\mathrm{cm}^{-3}$ and $\approx 3 \times 10^{18}\,\mathrm{cm}^{-3}$, respectively.

Figure 4 shows the scenario after the propagation of the main pulse beyond the focus in the two cases, ab-ASE (top of Fig. 4) and bb-ASE (bottom of Fig. 4), respectively. On top of Figure 4, the CPA pulse has interacted with the ASE pre-plasma (which has a density minimum on its axis, due to the expansion). The interaction splits the short pulse in two spatial components: the central one is collimated by the density channel on the axis; the other, ring shaped, is refracted away at an angle larger than the one of the focusing optics. Actually in the two-dimensional (2D) projection on the interferogram of the external plasma cone produced by this latter component, appears like two wings. The ASE plasma boundary of higher density (basically a shock wave expanding in the gas) is further ionized by the CPA pulse to higher electron density than the surrounding plasma. Completely different scenario is shown by the interferogram on the bottom of Fig. 4, in the case of *free propagation* (with no ASE pre-formed plasma). The emerging pulse keeps its original divergence due to the focusing optics.

To simulate the laser propagation through the gas jet and the electron density distribution resulting from the interaction, we used a numerical code based on the solution of the standard paraxial wave equation in cylindrical geometry. In the code, the equation of propagation is solved iteratively, and self-consistently with the ionization rate equations, on a (r, z) grid using a standard finite element method. The field-ionization is described either by a tunneling model (Gibbon *et al.*, 1995) or by Perelomov-Popov-Terent'ev formula (Ammosov *et al.*, 1986; Perelomov *et al.*, 1966, 1967), the latter being valid in both multi-photon and tunneling regimes of ionization. The results were found not to be

https://doi.org/10.1017/S0263034607000079 Published online by Cambridge University Press

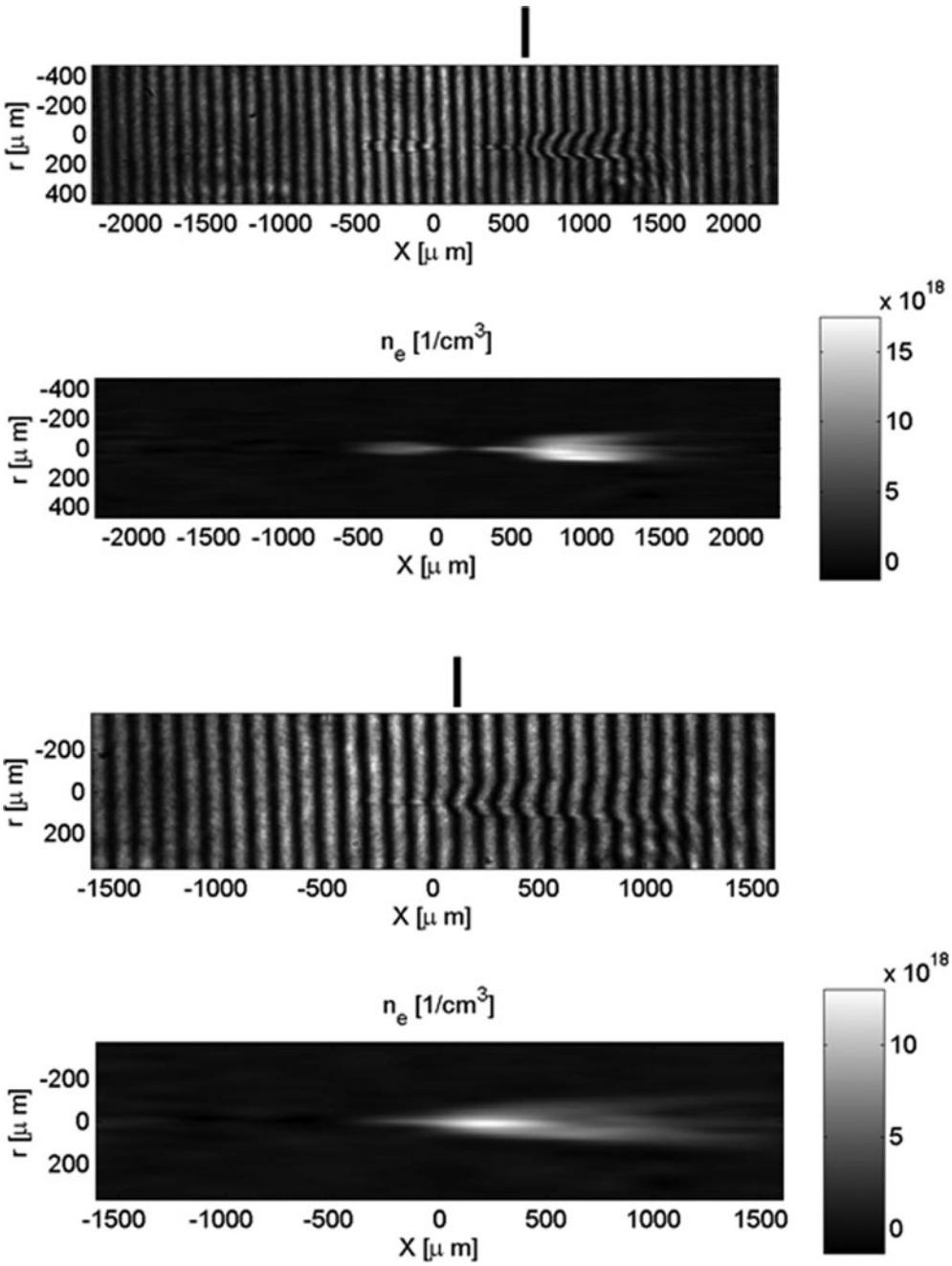

Fig. 3. Two interferograms (and retrieved electron density maps) showing the CPA pulse approaching the focus, nominally at $x = 0$. The gas is flowing from bottom. The laser light is coming from right. Vertical bars indicate the CPA pulse position. Top: the He density is *above* threshold for gas breakdown at the ASE intensity. Bottom: the He density is *below* threshold for gas breakdown at the ASE intensity.

sensitive to the different ionization rates. The ASE could not be included in the simulation, which can then be referred to all the bb-ASE data, and to the ab-ASE data only before the interaction of the main pulse with the ASE pre-plasma.

The history of the gas ionization during the propagation of the laser pulse with no ASE pre-plasma, as obtained from the numerical simulation, is shown in Figure 5, where the laser pulse comes now from the left-hand side. The simulation shows that the picosecond pedestal starts to ionize a few picoseconds before the femtosecond pulse reaches the nominal focus, i.e., the middle of the jet. The He pre-plasma produced in this way is singly ionized plasma, 20 μm in diameter, 300 μm in length. The simulation could not include the case of ASE preformed plasma. In general, the numerical data evidence a rather regular propagation only weakly affected by some refraction effect in this regime of intensity. There is a general agreement between simulation and experimental data as discussed in detail elsewhere (Giulietti *et al.*, 2006).

4. THE TRANSMITTED PULSE: SPATIAL DISTRIBUTION AND SPECTRUM

The laser light transmitted after the propagation in the gas was collected in a solid angle equal to the focusing one and used to: (1) produce the image of the laser focal spot;

https://doi.org/10.1017/S0263034607000079 Published online by Cambridge University Press

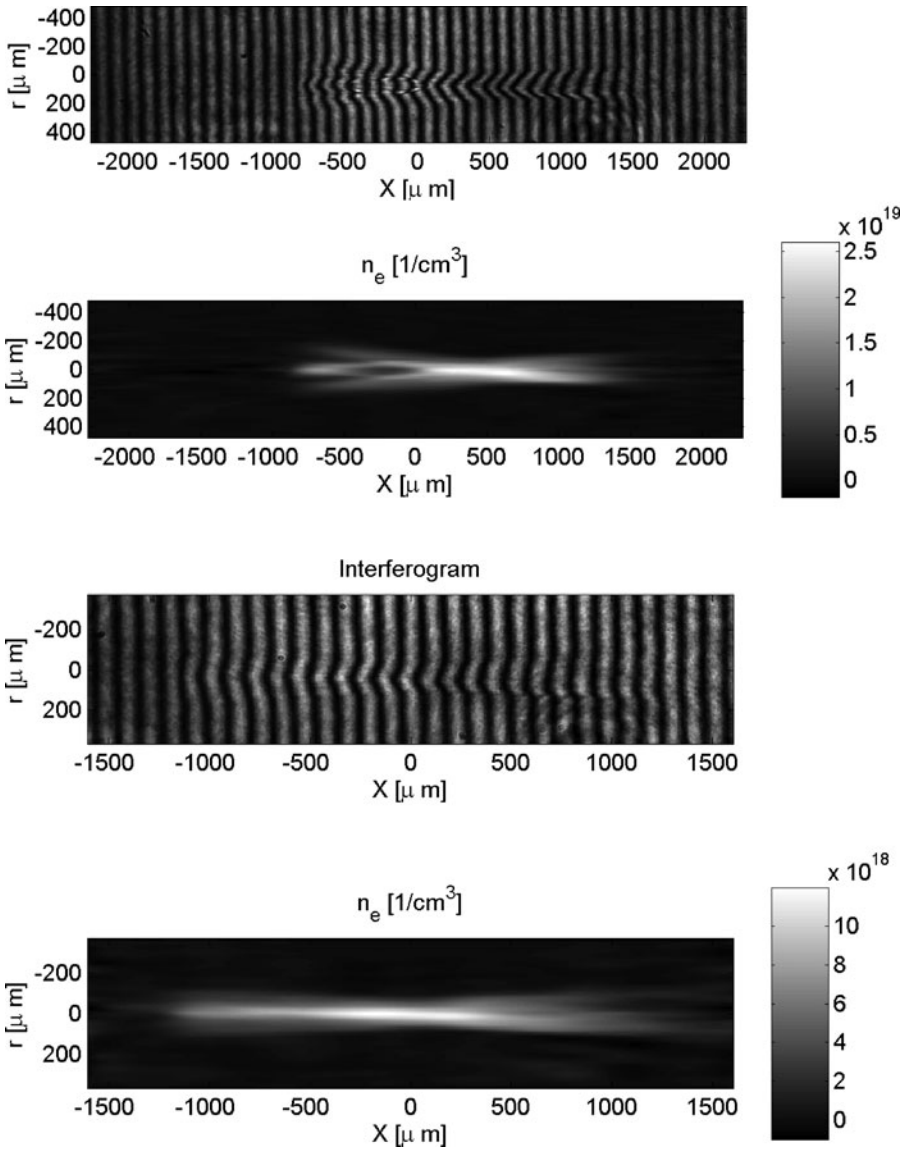

Fig. 4. Top: interferograms (and retrieved electron density map) obtained with He density *above* threshold for gas breakdown of ASE after the interaction between the CPA pulse coming from right and the plasma pre-formed by ASE. Bottom: interferogram (and retrieved electron density map) obtained with He density *below* threshold for gas breakdown of ASE after the propagation of the CPA pulse through the focal region.

(2) measure the fraction of laser light transmitted; (3) obtain the spectrum of the transmitted light. Images and spectra reproduced below are well representative of a number of reproducible data. The mean values for the parameters of the transmitted light (fraction of energy and peak intensity; spectral shift and broadening) are given in the Tables 1 and 2.

Figure 6 shows three-dimensional (3D) diagrams of the laser spot. The top diagram was obtained with no gas; the middle diagram in ab-ASE condition; the bottom diagram in bb-ASE condition. Table 1 shows the ratio of the transmitted energy and of the peak intensity to the corresponding quantities with no plasma.

From the plots of the laser spot, we see that the original laser spot has a definite amount of aberration resulting in an anomalous intensity distribution outside the main peak, which is substantially preserved after propagation with no ASE pre-formed plasma. This observation is also consistent with the transmission data for total energy and peak value. On the contrary, the interaction with the ASE preformed plasma acts on the CPA pulse as a spatial filter, allowing the propagation of a collimated, single-mode pulse, while scattering the wings out from the collected angle. This interesting effect is consistent with both transmission data (showing that total energy is three-four times more reduced than the peak energy) and interferometry (see top picture in

Table 1. *Fraction of the transmitted light and of the peak intensity with respect to the case of propagation in vacuum*

	Fraction of transmitted energy	Fraction of peak intensity
ASE preplasma	0.05 ± 0.04	0.18 ± 0.03
No preplasma	0.3 ± 0.15	0.31 ± 0.05

https://doi.org/10.1017/S0263034607000079 Published online by Cambridge University Press

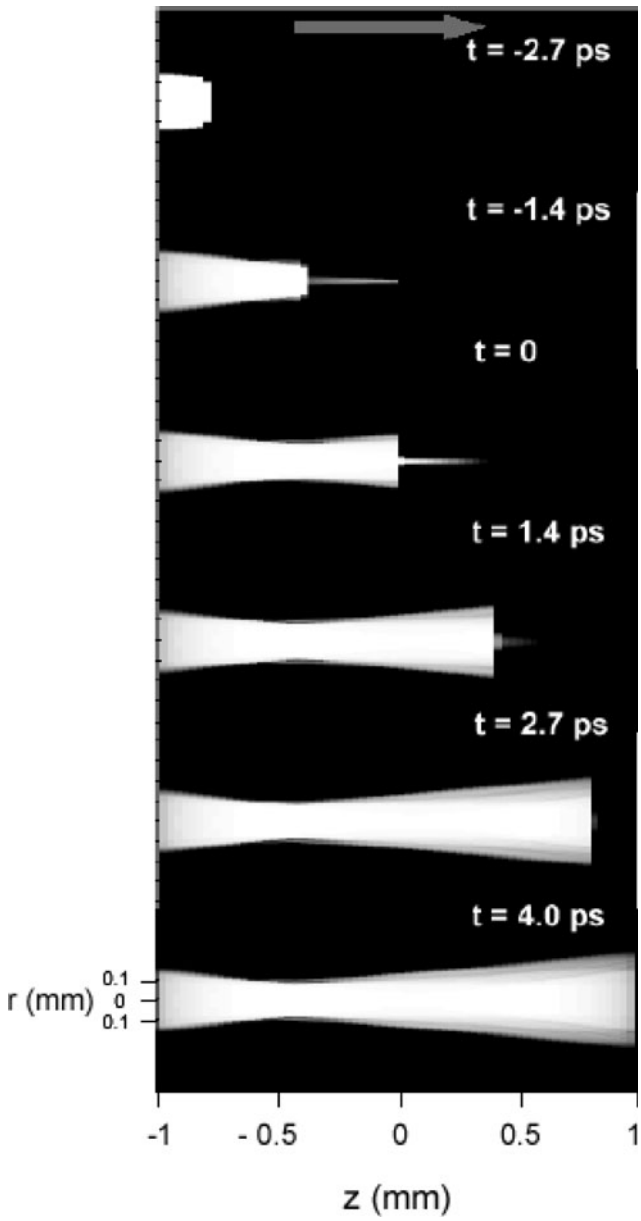

Fig. 5. A sequence of snap-shots from a numerical simulation performed in the same physical conditions of the experiment. The sequence shows the progressive ionization of the gas due to the propagation of the laser pulse. The ASE was not included in the simulation.

Fig. 4) showing the splitting of the CPA pulse in three parts (actually in a central beamlet plus an external corona). Spatial filtering of an ultra-short pulse by preformed plasma was already observed in the propagation through overdense foil plasma (Giulietti *et al.*, 1997).

The spectra of the transmitted light are plotted in Figure 7 in the three cases; no gas, ab-ASE and bb-ASE. The propagation in the gas produces in both cases (ab-ASE and bb-ASE) the same amount of blue shift and slight broadening to the main spectral component of the transmitted pulse. However, in the case of free propagation (bb-ASE), there is evidence for a broader blue shifted component with modulations not reproducible shot-to-shot. The maximum shift of this component is approximately constant in all the shots. A summary of the spectral data of the transmitted light is given in Table 2.

Table 2. *Spectral data of the transmitted light with respect to the propagation in vacuum*

	%Broadening	Shift (main component)	Maximum shift of the spectrum
ASE preplasma	50 ± 7	$\Delta\lambda = -15.0 \pm 2.6$ nm	
No preplasma	78 ± 12	$\Delta\lambda = -14.6 \pm 2.0$ nm	$\sim$95 nm

5. DISCUSSION AND PERSPECTIVES

The data from the transmitted light (the images and the spectrum of the pulse emerging from the plasma) can be understood if we consider that in the case of ASE preformed plasma, only the most intense central portion of the pulse contributes to images and spectra, since the outer part of

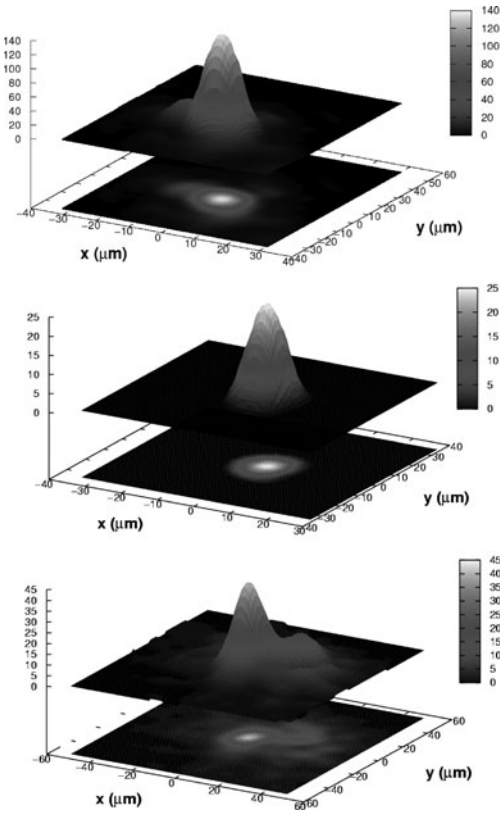

Fig. 6. 3D plots of the laser intensity distribution. Top: no gas. Middle: He density *above* threshold for gas breakdown of ASE. Bottom: He density *below* threshold for gas breakdown of ASE.

https://doi.org/10.1017/S0263034607000079 Published online by Cambridge University Press

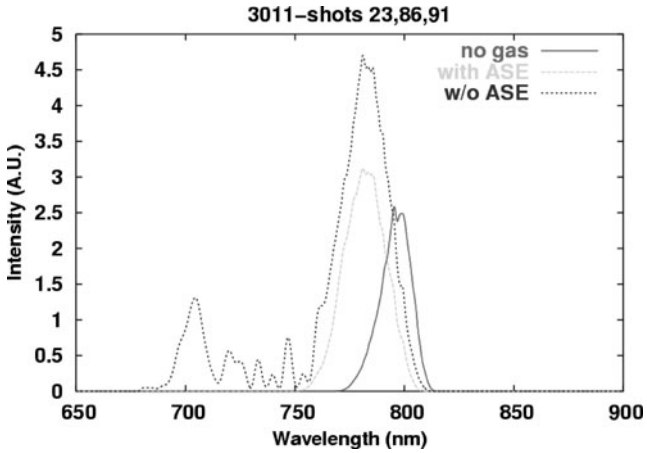

Fig. 7. Spectra of the transmitted laser light.

the pulse is refracted out from the imaging optics by the interaction with the ASE preformed plasma. On the contrary, in the case of no ASE preformed plasma, most of the transmitted pulse reaches the imaging optics and the spectrometer, thus allowing the information on the nonlinear effects affecting the pulse wings to be gained.

It is important to notice that the non-linear effects due to the laser ionization of the gas have a negligible effect on the most intense part of the pulse. In fact, in this region of the intensity distribution, ionization occurs in one or few optical cycles, and the rest of the pulse (more than 20 cycles in our case) will interact with fully ionized He. In this way, effects due to ionization, as defocusing or self-phase modulation (SPM) are ruled out from the propagation of the intense part of the focusing pulse. However, they can affect considerably the lateral wings of the pulse having lower levels of intensity, as well as the early and late pulse propagation out from the focal region, as confirmed also by the numerical simulation of the spectrum. This can explain the spectral component with larger shift and irreproducible modulations we have observed (Fig. 7) in the case of *free propagation*: we can attribute it to SPM of the wings of the pulse.

On the other hand, there was no evidence of a significant self-focusing of the pulse, in agreement with the numerical simulation. This is chiefly due to the weak relativistic intensity level of the laser pulse used in this experiment. This level of intensity has been thus proved to be substantially safe from severe effects and instabilities driven either by ionization (the intensity of the spatial and temporal "core" of the pulse is too high), or relativistic changes of the free electron mass (intensity too low) and then suitable for stable propagation in a low-Z gas at densities of interest for electron acceleration. This substantial stability remains also in presence of an ASE preformed plasma, which rather acts as a spatial filter on the pulse.

It may be attractive at this point, to extend the stable propagation of the pulse at constant intensity, to an optical path longer than the Raylegh range of the focusing optics. To this purpose, the gas jet described in Section 2 was characterized at the ILIL laboratory of IPCF/CNR in Pisa, where an investigation aimed at extending the propagation length of the focused pulse beyond the Rayleigh range of the focusing optics was performed. We used the well established data (Ostrovskaya & Zaidel, 1974) on optical gas breakdown by nanosecond laser pulses and subsequent evolution of the plasma in order to produce plasma channels.

The laser used for the plasma formation was a two beams Neodymium laser (YLF oscillator, phosphate glass amplifiers), wavelength 1053 nm, pulses of 3 ns FWHM. The laser operates in single longitudinal mode. One of the beams was used to produce the plasma and the other was devoted to the interferometry. The main beam was focused in a spot of 12 μm diameter by an $f/8$ lens in the gas-jet. We chose a particular range of energies: from 0.3 J to 0.5 J per pulse to be close to the intensity of a typical ASE pre-pulse.

A Nomarski interferometer (Benattar *et al.*, 1979; Squillacioti *et al.*, 2004) was used for observing interferometric images of the plasma; the fringes were recorded on a CCD camera. By changing the path of the probe beam by means of a sliding prism and so setting the delay with respect to the main beam, it was possible to study the plasma evolution. In this paper, we only consider interferograms obtained with a delay of 5 ns. The phase maps were deconvoluted using the same fringe analysis technique based on continuous wavelet transform ridge extraction (Tomassini *et al.*, 2001), and the improved Abel inversion algorithm (Tomassini & Giulietti, 2001) mentioned in Section 3. With that procedure we obtained the data on the electron density. A large number of interferograms were obtained with the setup described in Section 4. Many experimental parameters were varied in order to investigate different regimes (Gamucci *et al.*, 2006). Here we show in Figure 8 only an example of successful production of a plasma channel suitable for pulse guiding. The plasma was obtained focusing the main pulse in the centre of the gas jet with energy of 460 mJ in 3 ns which can simulate an ASE pre-pulse. From the fringe pattern on top of Figure 8 is already evident that long scale quasi-cylindrical plasma was produced. The electron density map in the middle of Figure 8 shows that the plasma has a minimum density on its axis: a plasma channel was produced. The diagram on the bottom of Figure 8 shows in turn the transversal density profile of the channel. This latter fits very well with the profile required for guiding (Durfee *et al.*, 1994; Leemans *et al.*, 1996) a pulse focused in a Gaussian spot of few 10 s of μm's. Focusing the nanosecond laser pulse in different positions of the gas jet we were able to produce channels with a variety of longitudinal density slopes (Gamucci *et al.*, 2006) so matching the requirements of specialized simulations (Sprangle *et al.*, 2001) for advanced acceleration schemes.

https://doi.org/10.1017/S0263034607000079 Published online by Cambridge University Press

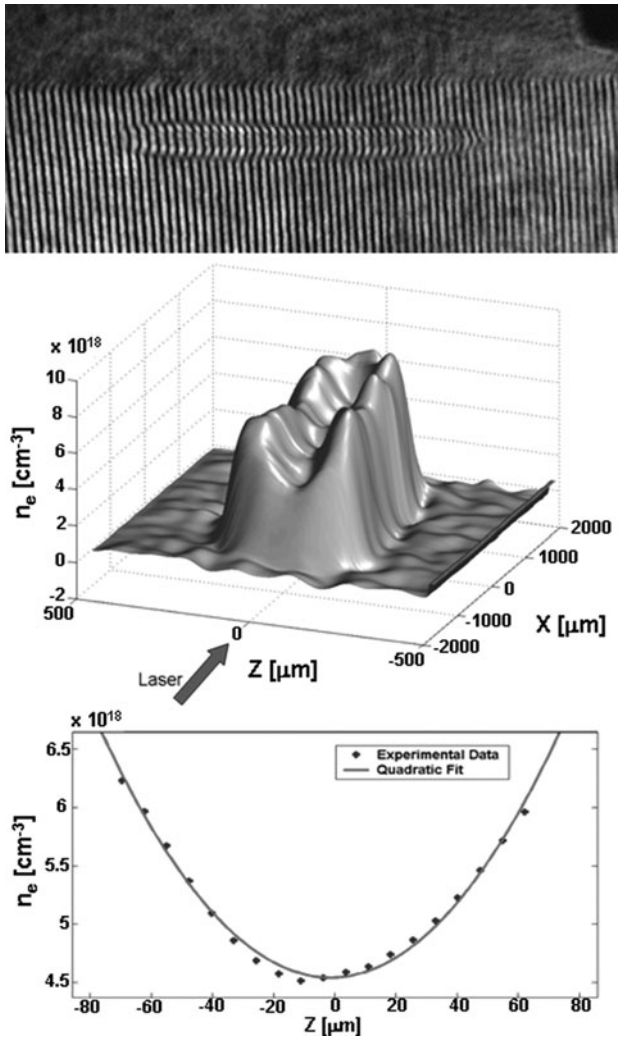

Fig. 8. A plasma channel produced with a ASE-like laser pulse in gas. Top: the interferogram. Middle: the electron density distribution; bottom: the transversal density profile.

6. CONCLUSION

In conclusion, the propagation of a moderately relativistic femtosecond CPA laser pulse in He, along a path length much larger than the focal depth, can be affected by early breakdown of the gas due to the ASE of the laser system. However, the interaction of the CPA pulse with the ASE preformed plasma is rather beneficial and results in a spatial filtering of the pulse itself, allowing the most intense part of the pulse to further propagate as a single mode beam. The outer part of the pulse is scattered out from the focusing cone. In the case of no early plasma production by ASE, the *free propagation* of the ASE pulse results in a higher level of transmission including also the pulse wings, these latter being in turn affected by non-linear effects, as well as the whole pulse before reaching the focal region. We have also evidences for the first time the plasma produced by the picosecond pedestal of the CPA pulse. This plasma precedes the main plasma in the focal region, just in front of the femtosecond pulse. The ionization data from which the propagation physics is inferred are in full agreement with the simulations obtained with a numerical code. Both experiment and simulation have shown that the effect of the picosecond precursor on the CPA propagation is not dramatic at this level of intensities. However, it has to be considered carefully in the future when designing experiments, as for laser acceleration in plasmas. We have thus characterized a favorable regime of propagation of intense ultrashort laser pulses in gases. This regime, suitable for many applications including high field electron acceleration by plasma waves, can be extended to propagation lengths much larger than the ones allowed by the focusing optics, with suitable guiding devices, including plasma channels, that we proved experimentally can be produced with precursor nanosecond laser pulses.

ACKNOWLEDGEMENTS

Authors acknowledge the technical support provided by both SLIC (CEA, Saclay) and ILIL (CNR, Pisa). The ILIL team stay at the SLIC laboratory was supported by the EU in the scheme for the access to the large facilities within the LASERNET network. This work was also partially supported by the Italian Ministry of University and Research with Funds for the Basic Research (Project BLISS) and by the National Institute of Nuclear Physics (Project PlasmonX).

REFERENCES

Ammosov, M.V., Delone, M.B. & Kraïnov, V.P. (1986). Tunnel ionization of complex atoms and atomic ions in an alternating electromagnetic field. *Sov. Phys. JETP* **64**, 1191.

Benattar, R., Popovics, C. & Sigel, R. (1979). Polarized light interferometer for laser fusion studies. *Rev. Sci. Instrum.* **50**, 1583.

Brambrink, E., Roth, M., Blazevic, A. & Schlegel, T. (2006). Modeling of the electrostatic sheath shape on the rear target surface in short-pulse laser-driven proton acceleration. *Laser Part. Beams* **24**, 163–168.

Chen, H. & Wilks, S.C. (2005). Evidence of enhanced effective hot electron temperatures in ultraintense laser-solid interactions due to reflexing. *Laser Part. Beams* **23**, 411–416.

Doumy, G., Quere, F., Gobert, O., Perdrix, M., Martin, P., Audebert, P., Gauthier, J.C., Geindre, J.-P. & Wittmann, T. (2004). Complete characterization of a plasma mirror for the production of high-contrast ultraintense laser pulses. *Phys. Rev. E* **69**, 026402

Duda, B.J., Hemker, R.G., Tzeng, K.C. & Mori, W.B. (1999). A long-wavelength hosing instability in laser-plasma interactions. *Phys. Rev. Lett.* **83**, 1978.

Durfee III., C.G., Linch, J. & Milchberg, H.M. (1994). Mode properties of a plasma waveguide for high-intensity laser pulses. *Opt. Lett.* **19**, 1937.

Faure, J., Glinec, Y. & Pukhov, A. (2004). A laser–plasma accelerator producing monoenergetic electron beams. *Nature* **431**, 541

Galimberti, M., Giulietti, A., Giulietti, D., Gizzi, L.A., Balcou, Ph., Rousse, A. & Rousseau, J.Ph. (2001). Investigation of

https://doi.org/10.1017/S0263034607000079 Published online by Cambridge University Press

femtosecond laser-plasma interactions through w and 2 w imaging and spectroscopy. *Laser Part. Beams* **19**, 47–53.

Gamucci, A., Galimberti, M., Giulietti, D., Gizzi, L.A., Labate, L., Petcu, C., Tomassini, P. & Giulietti, A. (2006). Production of hollow cylindrical plasmas for laser guiding in acceleration experiments. *Appl. Phys. B* **85**, 611–617.

Geddes, C.G.R., Toth, C.S. & Van, Tilborg, J. (2004). High-quality electron beams from a laser wakefield accelerator using plasma-channel guiding. *Nature* **431**, 538.

Gibbon, P., Monot, P., Auguste, R. & Mainfray, G. (1995). Measurable signatures of relativistic self-focusing in underdense plasmas. *Phys. Plasmas* **2**, 1305.

Giulietti, A., Tomassini, P., Galimberti, M., Giulietti, D., Gizzi, L.A., Koester, P., Labate, L., Ceccotti, T., D'Oliveira, P., Auguste, T., Monot, P. & Martin, P. (2006). Pre-pulse effect on intense femtosecond laser pulse propagation in gas. *Phys. Plasmas* **13**, 093103-1–093103-6.

Giulietti, D., Galimberti, M., Giulietti, A., Gizzi, L.A. & Tomassini, P., Borghesi, M., Malka, V., Fritzler, S., Pittman, M. & Taphouc, K. (2002). Production of ultracollimated bunches of multi-MeV electrons by 35 fs laser pulses propagating in exploding-foil plasmas. *Phys. Plasmas* **9**, 3655.

Giulietti, D., Gizzi, L.A., Giulietti, A., Macchi, A., Teychenné, D., Chessa, P., Rousse, A., Cheriaux, G., Chambaret, J.P. & Darpentigny, G. (1997). Observation of solid-density laminar plasma transparency to intense 30 femtosecond laser pulses. *Phys. Rev. Lett*. **79**, 3194.

Giulietti, D., Galimberti, M., Giulietti, A., Gizzi, LA., Labate, L. & Tomassini, P. (2005). The laser-matter interaction meets the high energy physics: Laser-plasma accelerators and bright X/gamma-ray sources. *Laser Part. Beams* **23**, 309–314.

Gizzi, L.A., Galimberti, M., Giulietti, A., Giulietti, D., Tomassini, P., Borghesi, M., Campbell, D.H., Schiavi, A. & Willi, O. (2001). Relativistic laser interactions with preformed plasma channels and gamma-ray measurements. *Laser Part. Beams* **19**, 47–53.

Glinec, Y., Faure, J., Pukhov, A., Kiselev, S., Gordienko, S., Mercier, B. & Malka, V. (2005). Generation of quasi-monoenergetic electron beams using ultrashort and ultraintense laser pulses. *Laser Part. Beams* **23**, 161–166.

Hidding, B., Amthor, K.-U., Liesfeld, B., Schwoerer, H., Karsch, S., Geissler, M., Veisz, L., Schmid, K., Gallacher, J.G., Jamison, S.P., Jaroszynski, D., Pretzler, G. & Sauerbrey, R. (2006). Generation of quasimonoenergetic electron bunches with 80-fs laser pulses. *Phys. Rev. Lett*. **96**, 105004.

Leemans, W.P., Siders, C.W., Esarey, E., Andreev, N.E., Shvets, G. & Mori, W.B. (1996). Plasma guiding and wakefield generation for second generation Experiments. *IEEE Trans. Plasma Sci.* **24**, 331.

Lifschitz, A.F., Faure, J., Glinec, Y., Malka, V. & Mora, P. (2006). Proposed scheme for compact GeV laser plasma accelerator. *Laser Part. Beams* **24**, 255–259.

Mangles, S.P.D., Murphy, C.D. & Najmudin, Z. (2004). Monoenergetic beams of relativistic electrons from intense laser–plasma interactions. *Nature* **431**, 535.

Mangles, S.P.D., Walton, B.R., Najmudin, Z., Dangor, A.E., Krushelnick, K., Malka, V., Manclossi, M., Lopes, N., Carias, C., Mendes, G. & Dorchies, F. (2006). Table-top laser-plasma acceleration as an electron radiography source. *Laser Part. Beams* **24**, 185–190.

Najmudin, Z., Krushelnik, K., Clark, E.L., Salvati, M., Santala, M.I.K., Tatarakis, M., Dangor, A.E., Malka, V., Neely, D., Allott, R. & Danson, C. (1999). First Observations of the laser hosing instability. CLF Annual Report 1998/99 Chien, UK: Rutherford Appleton Laboratory.

Ostrovskaya, G.V. & Zaidel, A.N. (1974). Laser spark in gases. *Sov Phys.-Usp*. **16**, 834.

Patin, D., Lefebvre, E., Bourdier, A. & D'Humieres, E. (2006). Stochastic heating in ultra high intensity laser-plasma interaction: Theory and PIC code simulations. *Laser Part. Beams* **24**, 223–230.

Perelomov, A.M., Popov, V.S. & Terent'ev, M.V. (1966). Ionization of atoms in an alternating electric field. *Sov. Phys. JETP* **23**, 924.

Perelomov, A.M., Popov, V.S. & Terent'ev, M.V. (1967). Ionization of atoms with electric ac fields. *Sov. Phys. JETP* **24**, 207.

Sheng, H., Kim, K.Y., Kumarappan, V., Layer, B.D. & Milchberg, H.M. (2005). Plasma wave guides efficiently generated by Bessel beams in elongated cluster gas jets. *Phys. Rev. E* **72**, 036411.

Sherlock, M., Bell, A.R. & Rozmus, W. (2006). Absorption of ultra-short laser pulses and particle transport in dense targets. *Laser Part. Beams* **24**, 231–234.

Sprangle, P., Hafizi, B., Peñano, J.R., Hubbard, R.F., Ting, A., Moore, C.I., Gordon, D.F., Zigler, A., Kaganovich, D. & Antonsen Jr., T.M. (2001). Wakefield generation and GeV acceleration in tapered plasma channels. *Phys. Rev. E* **63**, 056405.

Squillacioti, P., Galimberti, M., Labate, L., Tomassini, P., Giulietti, A., Shibkov, V. & Zamponi, F. (2004). Hydrodynamics of microplasmas from thin foils exploded by picosecond laser pulses. *Phys. Plasmas* **11**, 226.

Tomassini, P. & Giulietti, A. (2001). A generalization of Abel inversion to non-axisymmetric density distribution. *Opt. Commun.* **199**, 143.

Tomassini, P., Giulietti, A., Gizzi, L.A., Galimberti, M., Giulietti, D., Borghesi, M. & Willi, O. (2001). Analyzing laser plasma interferograms with a continuous wavelet transform ridge extraction technique: The method. *Appl. Opt.* **40**, 6561.

Wang, X., Nishikawa, K. & Nemoto, K. (2006). Observation of a quasimonoenergetic electron beam from a femtosecond prepulse-exploded foil. *Phys. Plasmas* **13**, 080702.